AMERICAN SOCIETY FOR MICROBIOLOGY | Infection and Immunity®

CELLULAR MICROBIOLOGY:
PATHOGEN-HOST CELL MOLECULAR INTERACTIONS

Peptoanaerobacter stomatis Primes Human Neutrophils and Induces Granule Exocytosis

E. Jimenez Flores,[a,c] S. Tian,[a] M. Sizova,[b]* S. S. Epstein,[b] R. J. Lamont,[c] S. M. Uriarte[a]

Department of Medicine, School of Medicine, University of Louisville, Louisville, Kentucky, USA[a]; Department of Biology, Northeastern University, Boston, Massachusetts, USA[b]; Department of Oral Immunology and Infectious Diseases, School of Dentistry, University of Louisville, Louisville, Kentucky, USA[c]

ABSTRACT *Peptoanaerobacter stomatis* is a newly appreciated taxon associated with periodontal diseases; however, little is known about the organism's pathogenic potential or its interaction with the host immune response. Neutrophils are the most abundant innate immune cell present in the gingival tissue and function to constrain the oral microbial challenge. However, some periodontal pathogens have developed strategies to evade phagocytosis and killing by neutrophils. Therefore, to begin to understand the role of *P. stomatis* in periodontitis, we studied its interactions with human neutrophils. Our data showed that after 30 min of incubation, neutrophils failed to engulf *P. stomatis* efficiently; however, when *P. stomatis* was internalized, it was promptly eradicated. *P. stomatis* challenge induced a robust intracellular respiratory burst; however, this response did not contribute to bacterial killing. Minimal superoxide release was observed by direct bacterial challenge; however, *P. stomatis* significantly increased *N*-formyl-methionyl-leucyl phenylalanine (fMLF)-stimulated superoxide release to an extent similar to that of cells primed with tumor necrosis factor alpha (TNF-α). When neutrophils were challenged with *P. stomatis*, 52% of the bacterium-containing phagosomes were enriched for the specific granule marker lactoferrin and 82% with the azurophil granule marker elastase. *P. stomatis* challenge stimulated exocytosis of the four neutrophil granule subtypes. Moreover, *P. stomatis* susceptibility to extracellular killing could be attributed to the exocytosis of antimicrobial components present in neutrophil granules. Priming neutrophils for an enhanced respiratory burst together with promoting granule content release could contribute to the chronic inflammation and tissue destruction that characterize periodontal diseases.

KEYWORDS *Peptoanaerobacter stomatis*, periodontitis, killing mechanisms, neutrophil, periodontal immunology

Received 20 December 2016 **Returned for modification** 14 February 2017 **Accepted** 18 April 2017

Accepted manuscript posted online 24 April 2017

Citation Jimenez Flores E, Tian S, Sizova M, Epstein SS, Lamont RJ, Uriarte SM. 2017. *Peptoanaerobacter stomatis* primes human neutrophils and induces granule exocytosis. Infect Immun 85:e01043-16. https://doi.org/10.1128/IAI.01043-16.

Editor Beth McCormick, University of Massachusetts Medical School

Address correspondence to R. J. Lamont, rich.lamont@louisville.edu, or S. M. Uriarte, silvia.uriarte@louisville.edu.

* Present address: M. Sizova, Evelo Biosciences, Cambridge, Massachusetts, USA.

Periodontal diseases are one of the most prevalent infectious diseases worldwide, affecting almost one-half of the U.S. population (1). These disorders lead to destruction of the hard and soft tissues of the periodontium (2, 3) and are also associated with serious systemic conditions such as rheumatoid arthritis, cardiovascular disease, diabetes, and adverse pregnancy outcomes (4–6). Periodontitis is a polymicrobial chronic inflammatory disease, and the understanding of the disease etiology developed through the extensive study of a limited number of species, including *Porphyromonas gingivalis*, *Tannerella forsythia*, and *Treponema denticola* (7, 8). More recently, culture-independent techniques have identified a variety of other bacterial species that increase in number in disease (9). *Peptoanaerobacter stomatis* is one such newly appreciated potential oral pathogen that is present in oral biofilms in patients with periodontal diseases in higher numbers than in healthy individuals (10–12). Sizova et al. (12) classified this organism as a novel genus and species within the family of

Peptostreptococcaceae, and *P. stomatis* represents the first known cultivable member of the human oral taxon 081 (13). *P. stomatis* is a Gram-positive obligate anaerobic rod with round ends, with a diameter of 0.5 to 0.7 μm and a length of 1.0 to 2.3 μm, often forming chains (12), and highly motile due to peritrichous flagella (14). In addition to periodontitis, *P. stomatis* is associated with dentoalveolar abscesses and endodontic infections (14).

As a major component of the innate host response, neutrophils contribute to the maintenance of a healthy gingival crevice (15, 16). Following phagocytosis, bacteria are killed by oxygen-dependent and -independent mechanisms, which can also act on extracellular microorganisms (17, 18). While the generation of high concentrations of reactive oxygen species (ROS), such as superoxide ion (O_2^-), is a key antimicrobial feature (19), if this response is not regulated properly, it can lead to severe tissue destruction of the periodontium, characteristic of periodontal disease (2). Another neutrophil killing mechanism, which does not involve oxygen consumption, involves mobilization of neutrophil granule subtypes (18). Upon activation, these granules fuse with the phagosome or the plasma membrane, releasing their antimicrobial components either inside the bacterium-containing phagosome or to the extracellular environment (21). The components of the secretory vesicles and the gelatinase granules also aid in early neutrophil mechanisms such as adhesion, migration, chemotaxis, and extravasation; therefore, they are the first to undergo exocytosis (22, 23). The last granules to be mobilized are the specific and azurophil granules, which contribute to phagosome maturation and contain the most microbicidal and cytotoxic components (24, 25).

In this study, we demonstrate that neutrophils have a low phagocytic ability toward *P. stomatis*, with 22% of the bacteria internalized after 30 min of challenge. However, once *P. stomatis* is internalized, it is eradicated efficiently in an ROS-independent manner. More than 65% of *P. stomatis* remains attached to the neutrophil plasma membrane, which might contribute to priming of *N*-formyl-methionyl-leucyl phenylalanine (fMLF)-stimulated superoxide release. In addition, *P. stomatis* induced robust exocytosis of the four neutrophil granule subtypes.

RESULTS

Neutrophils have a low phagocytic efficiency for *P. stomatis*. High numbers of neutrophils are recruited to the gingival tissue and the gingival crevice, where they phagocytose and destroy periodontal bacteria (2, 16). Successful periodontal pathogens, however, can resist neutrophil killing mechanisms. For example, the keystone pathogen, *P. gingivalis*, prevents neutrophil phagocytosis by a complex signaling mechanism that involves activation and cross talk between C5aR and Toll-like receptor 2 (TLR2), leading to suppression of actin polymerization (36). To assess the susceptibility or recalcitrance of *P. stomatis* to neutrophil phagocytosis, engulfment of carboxyfluorescein succinimidyl ester (CFSE)-labeled *P. stomatis* was measured by imaging flow cytometry (Fig. 1A). Under the control condition, 45 to 50% of neutrophils internalized *Staphylococcus aureus* after a 30-min challenge, consistent with previous reports (30) (Fig. 1B). However, only 22% of the neutrophils internalized *P. stomatis* after 30 min, with a modest, nonsignificant increase after 120 min of challenge (Fig. 1B). Since serum opsonization increases neutrophils' phagocytic ability, cells were challenged with serum-opsonized *P. stomatis*. A similar level of CFSE-positive neutrophils, less than 25%, was observed with both opsonized as well as nonopsonized *P. stomatis* (Fig. 1C). Hence, all further experiments were conducted with nonopsonized bacteria.

To confirm the low phagocytic ability of neutrophils toward *P. stomatis* and to distinguish between surface-associated bacteria and fully engulfed bacteria, the neutrophil plasma membrane was stained with wheat germ agglutinin (WGA) prior to bacterial challenge. Confocal microscopy showed that, similar to the data obtained by imaging flow cytometry, at a multiplicity of infection (MOI) of 10, only 11% of neutrophils had fully engulfed the bacteria and 25% of the cells had both surface-bound and

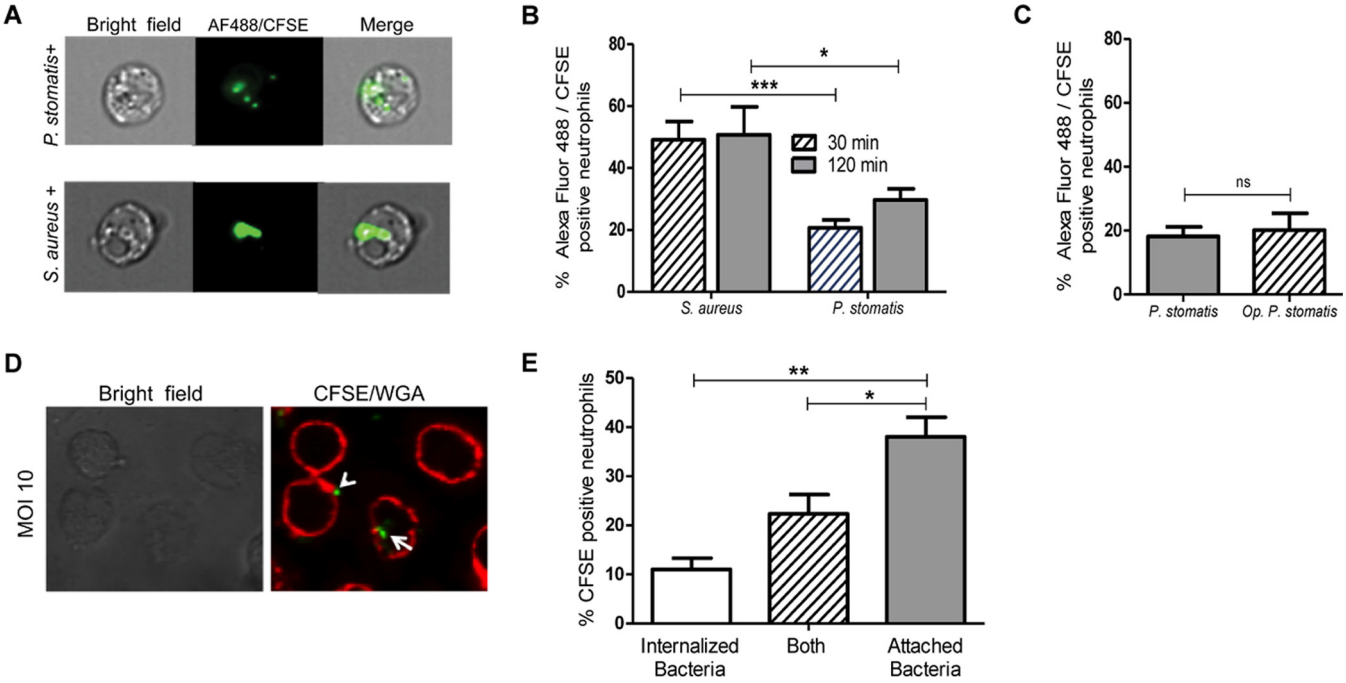

FIG 1 *P. stomatis* and human neutrophil interaction. Neutrophils were challenged with Alexa Fluor 488 *S. aureus*, opsonized CFSE-labeled *P. stomatis* (Op *P. stomatis*), or nonopsonized CFSE-labeled *P. stomatis* (*P. stomatis*) for 30 or 120 min. After the 30 min (A to C) or 120 min (A and B) of bacterial challenge, cells were visualized and quantified via ImageStreamX flow cytometry. One thousand neutrophil events were collected and sorted into bacterium-positive or -negative bins based on CFSE/Alexa Fluor 488 intensity and a mask designed to ignore signals from associated or extracellular bacteria. Data are expressed as the means ± standard errors of the means (SEM) of the percentage of bacterium-positive neutrophils from 6 independent experiments. (D) Representative confocal image of WGA-stained neutrophil membrane and CFSE-labeled *P. stomatis* after 30 min of challenge. (E) Percentage of CFSE-positive neutrophils with internalized-only, attached/internalized (Both), or attached-only *P. stomatis*. Data are expressed as means ± SEM of percentages of CFSE-positive neutrophils from 3 separate experiments. *, $P < 0.05$; **, $P < 0.001$; ***, $P < 0.0001$.

engulfed bacteria, with the majority of the neutrophils showing surface-bound bacteria only (Fig. 1D and E).

Bacterial viability upon neutrophil challenge. The data in Fig. 1 show that *P. stomatis* is more resistant to neutrophil phagocytosis than is *S. aureus*. Therefore, the next step was to determine the extent to which internalized organisms are killed by neutrophils. Plate counting for *P. stomatis* results in a very low percent recovery, so to overcome this limitation, Baclight staining was used to determine bacterial viability (21). Neutrophils were challenged with *P. stomatis*, and bacterial viability was determined using DAPI (4′,6-diamidino-2-phenylindole) for intact bacteria and Sytox Green for bacteria with compromised membranes (Fig. 2A). After 30 min of *P. stomatis* challenge, 87% of the extracellular bacteria were viable, 70% of the plasma membrane-bound bacteria were viable, and 42% of the internalized bacteria were viable (Fig. 2B). In contrast, after 120 min of neutrophil challenge, bacterial survival decreased significantly compared to the 30-min challenge, with 28% of bacteria remaining viable either extracellularly or as membrane-bound or internalized bacteria (Fig. 2C). The percent viabilities of the bacterial inocula used for the assays were 90% for 30 min and 87% for 120 min (Fig. 2D). After a longer incubation time with neutrophils, the survival rates of both extracellular and internalized bacteria are significantly reduced. However, 25 to 28% of the bacteria after 2 h of exposure to the neutrophils are able to resist killing by neutrophils.

***P. stomatis* induces a robust neutrophil respiratory burst response, which did not contribute to bacterial killing.** Upon recognition and binding of bacteria, neutrophils initiate the phagocytic process, which is accompanied by assembly and activation of the NADPH oxidase complex, with reduction of oxygen and generation of high levels of reactive oxygen species within the phagosome (19, 29). Bacterial pathogens can manipulate the respiratory burst response as a way to withstand neutrophil

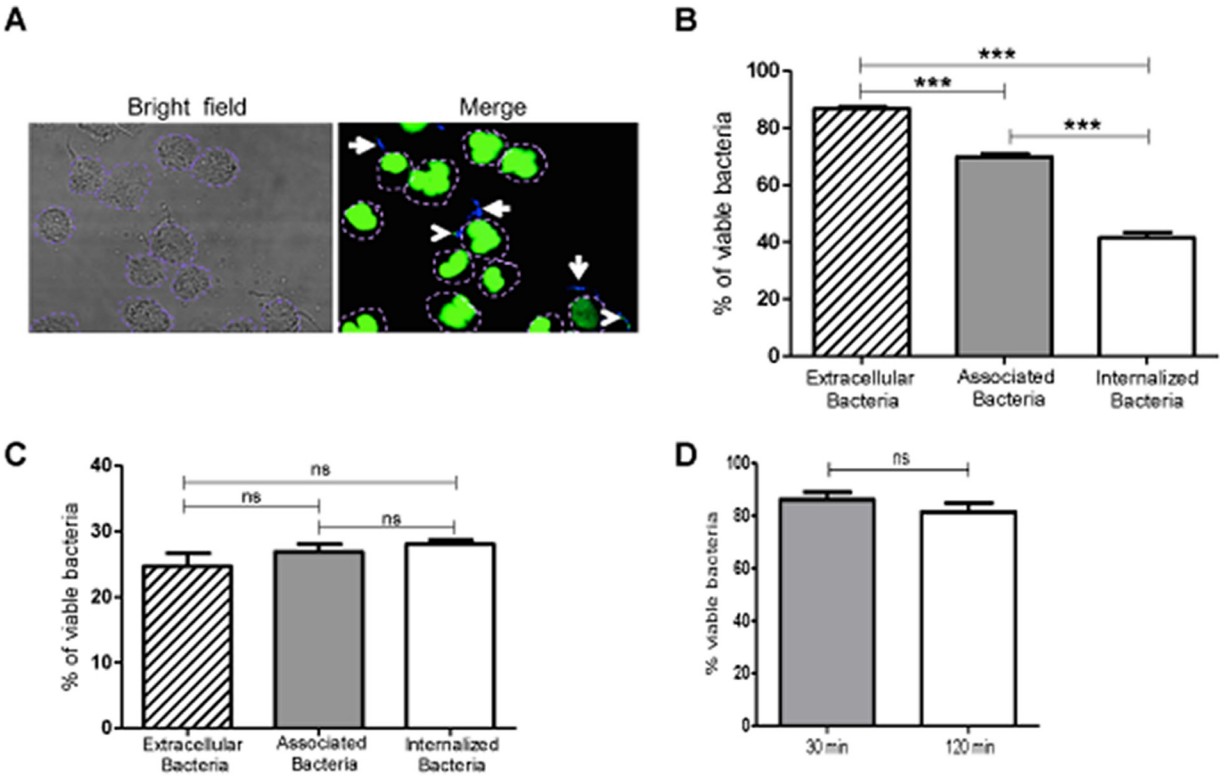

FIG 2 *P. stomatis* viability after neutrophil challenge. Neutrophils were challenged with DAPI-labeled *P. stomatis* (MOI, 10) for 30 or 120 min. Viable (blue) and nonviable (green/turquoise) *P. stomatis* strains were distinguished using BacLight DNA dyes DAPI and Sytox Green. (A) Representative confocal image, where white arrows indicate viable *P. stomatis* (blue) and arrowheads indicate nonviable *P. stomatis* (green/turquoise). A dashed purple line is drawn to delineate the neutrophil plasma membrane. (B and C) The percentages of viable *P. stomatis* cells that were internalized, associated, or extracellular were quantified from 200 neutrophils after 30 min (B) and 120 min (C) of neutrophil challenge (means ± SEM from 3 independent experiments). (D) Viability of *P. stomatis* inoculum after 30 or 120 min of exposure to the same experimental conditions as when incubated with the neutrophils. ***, $P < 0.0001$; ns, nonsignificant.

killing mechanisms. A nitroblue tetrazolium (NBT) assay was utilized to localize ROS accumulation inside *P. stomatis* phagosomes (29). Minimal blue deposits were observed in unstimulated neutrophils, whereas defined blue deposits accumulated in both *S. aureus* and *P. stomatis* phagosomes (Fig. 3A). To quantify intracellular ROS generation, neutrophils were challenged with either *S. aureus* or *P. stomatis*, and intracellular ROS production was analyzed by flow cytometry. As shown in Fig. 3B, *P. stomatis* induced a time-dependent increase in intracellular ROS production that was significantly higher than the response to *S. aureus* after 30 min of bacterial challenge.

Depending on the stimuli, neutrophils can also assemble the NADPH oxidase at the plasma membrane, and consequently, the ROS generated is released outside the cell (29). Next, we examined if *P. stomatis* challenge would also induce extracellular ROS. Unlike intracellular ROS, the *P. stomatis*-challenged neutrophils showed minimal superoxide release, which was similar to basal levels from unstimulated cells (Fig. 3C).

The degree of neutrophil activation is tightly regulated due to the deleterious consequences that a fully activated cell can have on host tissue. Neutrophils can display a minimal degree of activation upon exposure to an agonist but will exhibit an enhanced response upon exposure to a second stimulus, a phenotype known as priming. Circulating neutrophils as well as cells isolated from the oral cavity from chronic periodontitis patients have a primed phenotype (27, 32). Our data indicate that more than 65% of *P. stomatis* cells remain associated with the neutrophil surface without inducing extracellular release of ROS. To examine the ability of *P. stomatis* to prime neutrophils, cells were first exposed to *P. stomatis* for 10 min, followed by a second stimulus of fMLF. Similar to the control tumor necrosis factor alpha (TNF-α)-induced priming of the respiratory burst response, preexposure of neutrophils to *P. stomatis* significantly

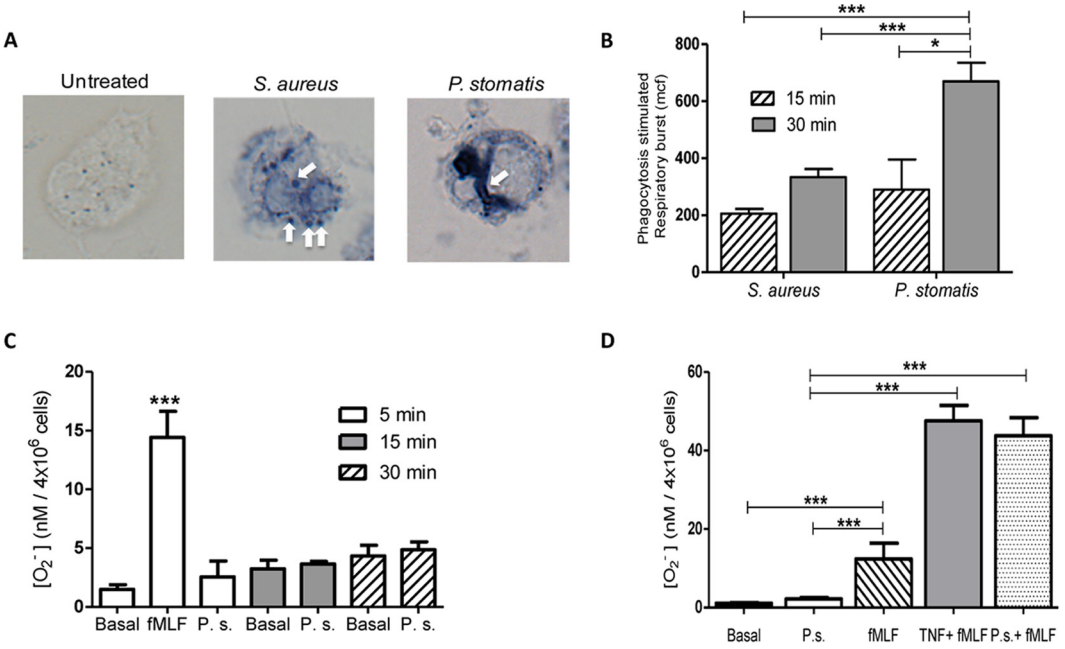

FIG 3 Neutrophil respiratory burst response to *P. stomatis* challenge. (A) Neutrophils were untreated or challenged with *S. aureus* or *P. stomatis* for 30 min, and intracellular superoxide production was detected by the presence of blue formazan deposits by NBT assay. Images were analyzed by light microscopy. White arrows depict NBT-positive phagosomes. (B) Neutrophils were challenged with *S. aureus* or *P. stomatis* for 15 or 30 min, and the intracellular respiratory burst response was analyzed by measuring the change of fluorescence after oxidation of dichlorofluorescein diacetate (DCF) by flow cytometry. Basal DCF levels from unstimulated cells were subtracted from the corresponding stimulation levels. Data are expressed as means ± SEM of the mean channel of fluorescence (mcf) from 5 independent experiments. (C) Neutrophils were unchallenged (Basal), stimulated with fMLF, or challenged with *P. stomatis* (P.s.) for 5, 15, and 30 min. Following stimulation, extracellular production of superoxide was measured by the colorimetric reduction of ferricytochrome *c*. Data are expressed as the means ± SEM of $[O_2^-]$ nanomoles per 4×10^6 cells released from 3 independent experiments. (D) Neutrophils were unchallenged (Basal), stimulated with fMLF, or pretreated with TNF-α followed by fMLF stimulation (TNF-α + fMLF), or challenged with *P. stomatis* (P.s.), or challenged with *P. stomatis* followed by fMLF stimulation (P.s. + fMLF). Following the different stimulations, extracellular production of superoxide was measured by the colorimetric reduction of ferricytochrome *c*. Data are expressed as the means ± SEM of $[O_2^-]$ nanomoles per 4×10^6 cells released from 5 independent experiments. *, $P < 0.05$; **, $P < 0.001$; ***, $P < 0.0001$.

enhanced the fMLF-stimulated superoxide release (Fig. 3D). *P. stomatis* on its own did not trigger superoxide release, a phenotype shared by all priming agents (33, 34). Collectively, these results indicate that *P. stomatis* induces a robust intracellular ROS production with minimal activation of the NADPH oxidase at the neutrophil plasma membrane. However, *P. stomatis* can prime the neutrophils for fMLF-stimulated superoxide release.

To address whether the robust intracellular ROS induced upon *P. stomatis* challenge contributes to bacteria killing, an inhibitor of the NADPH oxidase activity, diphenyleneiodonium (DPI), was used. After 30 min of exposure to human neutrophils, this set of donors showed that 31% of the internalized *P. stomatis* organisms and between 81% of the extracellular bacteria remained viable as determined by BacLight (Fig. 4A and B). Blocking the NADPH oxidase with DPI did not increase *P. stomatis* intracellular or extracellular survival after 30 min of bacterial challenge (Fig. 4A and B). In addition, DPI treatment did not affect *P. stomatis* survival (data not shown). However, DPI significantly reduced *P. stomatis*-induced intracellular ROS production (Fig. 4C), suggesting that at the 30-min time point, the respiratory burst response is not the major antimicrobial weapon used by neutrophils to effectively kill *P. stomatis*. However, we observed a significant decrease of *P. stomatis* extracellular survival after 120 min (Fig. 2C). *P. stomatis* induced minimal extracellular superoxide release after 120 min of neutrophil challenge (data not shown). To determine if the minimal amount of superoxide released after 120 min of neutrophil challenge could contribute to the significant extracellular bacterial killing, neutrophils from a patient with autosomal chronic gran-

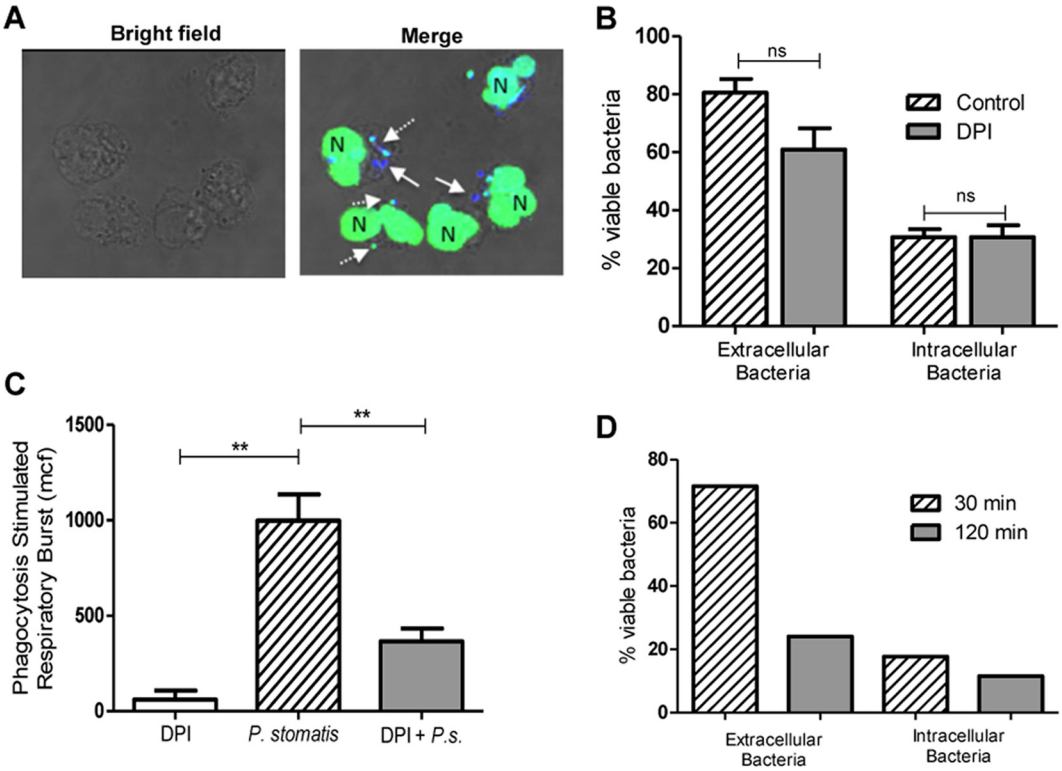

FIG 4 Killing of *P. stomatis* is ROS independent. Neutrophils were challenged with *P. stomatis* (30 min) in the presence or absence of DPI (10 μM). (A) Representative confocal image of viable (blue) and nonviable (green/turquoise) *P. stomatis* strains, which were distinguished by using the BacLight viability dyes DAPI and Sytox Green. White arrows indicate viable intracellular bacteria; the dashed white arrows indicate dead intracellular bacteria. N, neutrophil nucleus. (B) Percentage of viable extracellular (external) and intracellular (internal) bacteria from 200 neutrophils with and without DPI from 3 independent experiments. ns, nonsignificant. (C) Neutrophils were challenged with *P. stomatis* (30 min), with *P. stomatis* + DPI (P.s. + DPI), or with DPI alone. Intracellular ROS production was measured by flow cytometry as described above. Data are expressed as means ± SEM of the mean channel of fluorescence (mcf) from 3 independent experiments. **, $P < 0.001$. (D) CGD patient neutrophils were challenged with DAPI-labeled *P. stomatis* for 30 or 120 min, and bacterial viability was determined using the BacLight assay. The percentage of viable extracellular (external) and intracellular (internal) bacteria from 200 CGD neutrophils was determined for each time point.

ulomatous disease (CGD), with impaired oxidase function, were challenged with *P. stomatis* for 30 and 120 min, and bacterial survival was determined by BacLight. CGD patient neutrophils showed a similar ability to kill extracellular and intracellular *P. stomatis* isolates, as observed with neutrophils from healthy donors. After 30 min of *P. stomatis* challenge of CGD neutrophils, 70% of extracellular bacteria were viable, and by 120 min only 21% of extracellular bacteria survived (Fig. 4D). Collectively, these results strongly indicate that the ability of neutrophils to kill extracellular as well as intracellular *P. stomatis* is ROS independent.

***P. stomatis* phagosomes are enriched with both specific and azurophil granules.** Specific and azurophil granule fusion to bacterium-containing phagosomes is crucial for optimal respiratory burst responses and for phagosome maturation and efficient bacterial killing (19). The recruitment of specific and azurophil granules to *S. aureus* or *P. stomatis* phagosomes was examined by immunostaining against each granule subtype content protein, lactoferrin and elastase, respectively, and analyzed by confocal microscopy. Under the control condition, more than 60% of *S. aureus* phagosomes were enriched for the specific granule protein, lactoferrin, after 30 min of neutrophil challenge (Fig. 5A and B). In neutrophils challenged with *P. stomatis*, 53% of the phagosomes were enriched for lactoferrin (Fig. 5A and B). *P. stomatis* phagosomes were highly enriched for the azurophil granule protein, elastase, after 30 min of neutrophil challenge, similar to what was seen in the control with *S. aureus* (Fig. 5C and D). These results show that neutrophil-specific and azurophil granules fuse with *P. stomatis*-containing phagosomes.

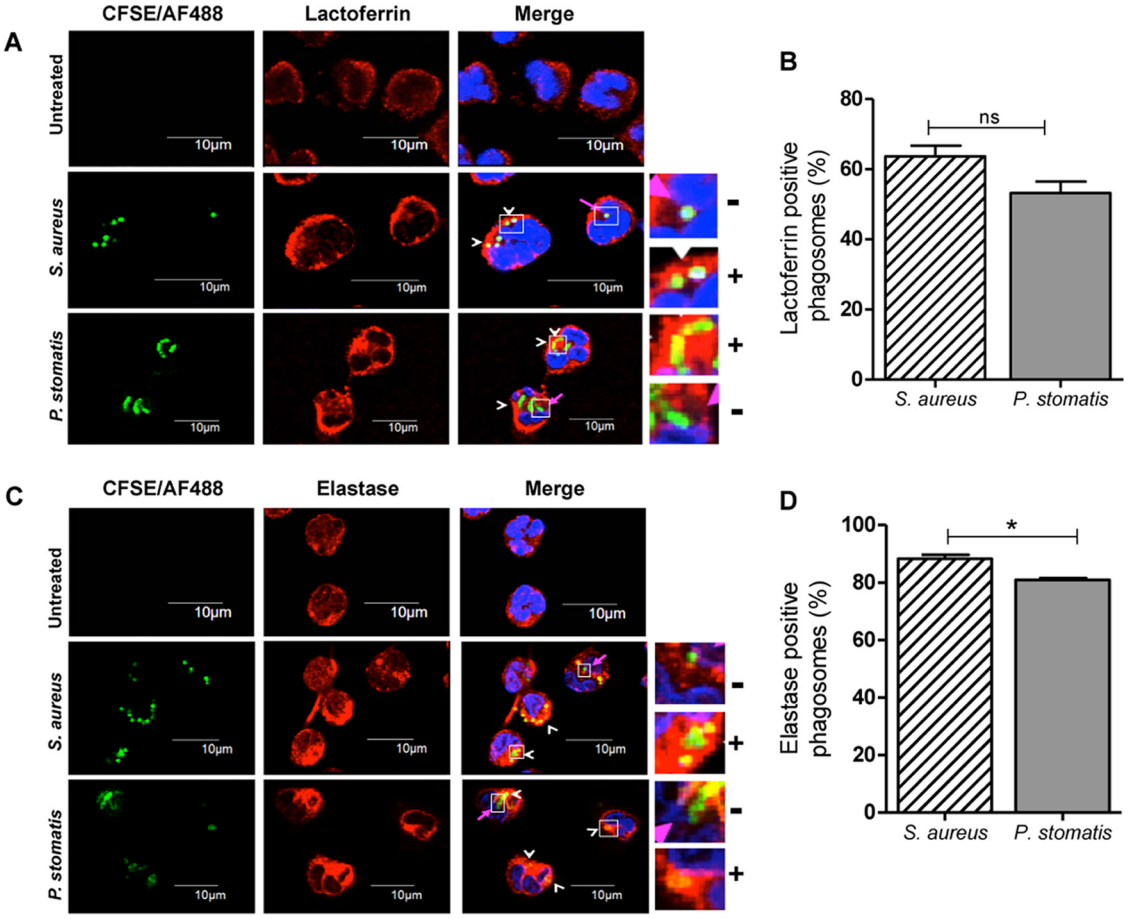

FIG 5 Both specific and azurophil granules are recruited to *P. stomatis* phagosomes. Neutrophils were unchallenged or challenged with CFSE-labeled *P. stomatis* (30 min) or with Alexa Fluor 488-labeled *S. aureus* (30 min). (A) Following the corresponding incubation time, cells were fixed, permeabilized, and stained with the specific granule marker lactoferrin to visualize its recruitment to the bacterium-containing phagosomes by confocal microscopy. Lactoferrin-positive (+) or -negative (−) enrichment to either *S. aureus* or *P. stomatis* phagosomes is shown in the inset. (B) Approximately 100 infected cells per condition were examined, and phagosomes were labeled as lactoferrin positive if ≥50% of the phagosome was surrounded by the granule marker. White arrowheads show lactoferrin-positive phagosomes, and pink arrows show lactoferrin-negative phagosomes. Data are expressed as the means ± SEM of the percentage of lactoferrin-positive phagosomes from 4 independent experiments. (C) Following the corresponding incubation time, cells were fixed, permeabilized, and stained with the azurophil granule marker elastase to visualize its recruitment to the bacterium-containing phagosomes by confocal microscopy. Elastase-positive (+) or -negative (−) enrichment to either *S. aureus* or *P. stomatis* phagosomes is shown in the inset. (D) Approximately 100 infected cells per condition were examined, and phagosomes were labeled as elastase positive if ≥50% of the phagosome was surrounded by the granule marker. White arrowheads show elastase-positive phagosomes, and pink arrows show elastase-negative phagosomes. Data are expressed as the means ± SEM of the percentages of lactoferrin-positive phagosomes from 3 independent experiments. DAPI (blue) was used to stain the neutrophil nucleus. ns, nonsignificant. *, $P < 0.05$.

***P. stomatis* induces robust neutrophil granule exocytosis.** Our data thus far showed that *P. stomatis* is resistant to internalization by human neutrophils and that the low numbers of this bacterium that are engulfed are killed independently of ROS, resulting mainly from phagosome maturation. However, *P. stomatis* induced robust intracellular ROS production and was able to prime neutrophils for a significant release of superoxide radicals upon subsequent stimulation with a formylated bacterial peptide. Hence, we wanted to determine if *P. stomatis* would induce neutrophil activation through promoting granule exocytosis. Stimulation of human neutrophils with *P. stomatis* resulted in a robust secretory vesicle exocytosis, which was significantly higher than the response induced by fMLF (Fig. 6A). To determine if *P. stomatis*-induced granule mobilization was comparable to the response induced by other oral bacteria, neutrophils were challenged with *P. gingivalis*. Our data show that *P. stomatis* mobilization of secretory vesicles was similar to the response induced by *P. gingivalis* (Fig. 6B). In addition, significantly higher levels of MMP-9, a protein found within gelatinase

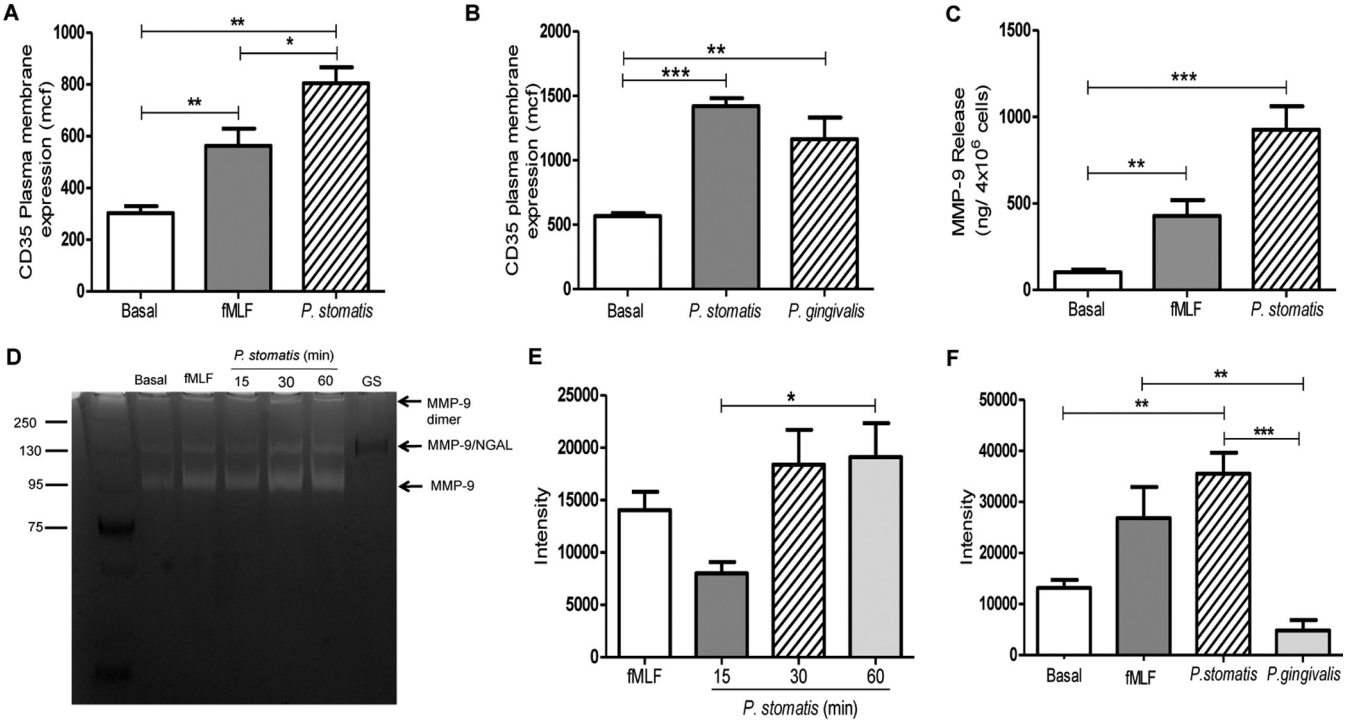

FIG 6 (A) *P. stomatis* induces the exocytosis of secretory vesicles and gelatinase granules. Neutrophils were unchallenged (basal) or challenged with fMLF (5 min), with *P. stomatis* (30 min), or with *P. gingivalis* (30 min). (A and B) Secretory vesicle exocytosis was determined by the increase in plasma membrane expression of CD35 by flow cytometry. Data are expressed as the means ± SEM of the mean channel of fluorescence (mcf) from 3 independent experiments. (C) Gelatinase granule exocytosis was measured as levels of matrix metalloproteinase 9 (MMP-9) present in the supernatants collected from the different experimental conditions by ELISA. Data are expressed as means ± SEM of MMP-9 release (in nanograms per 4×10^6 cells) from 4 independent experiments. (D) The activities of MMP-9 on the supernatants from the same experimental conditions were analyzed by gelatin zymogen assays. The supernatant from *P. stomatis* growth media (GS) was also analyzed. The protein standard is shown on the left. MMP-9 isoforms are indicated. (E and F) The densitometry profile of the degraded gelatin zymography 92-kDa band was analyzed by ImageJ software from the gels of 4 independent experiments (E) or from 3 independent experiments (F). *, $P < 0.05$; **, $P < 0.001$; ***, $P < 0.0001$.

granules, were induced upon *P. stomatis* challenge than with fMLF (Fig. 6C). To determine if *P. stomatis* induction of gelatinase granule exocytosis resulted in the extracellular release of active matrix metalloproteinases, supernatants collected from *P. stomatis*-challenged neutrophils were analyzed by gelatin zymography. Figure 6D and E show prominent bands at 92 kDa, the corresponding molecular mass of MMP-9, for the positive control and for fMLF- and *P. stomatis*-stimulated neutrophils. In addition, a higher-molecular-mass band, around 130 kDa, was also observed under the *P. stomatis* supernatant conditions, which might correspond to an MMP-9 dimer with neutrophil gelatinase-associated lipocalin (NGAL) as previously reported (35). In contrast, the supernatants collected from *P. gingivalis*-challenged human neutrophils showed a significantly lower band intensity at 92 kDa when analyzed by gelatin zymography (Fig. 6F). No bands were observed when the supernatant from *P. stomatis* culture was examined by zymography (Fig. 6D), indicating that gelatinase activity originates from the neutrophils.

The release of neutrophil granules is hierarchical, requiring stronger stimuli to induce mobilization of specific and azurophil granules than for secretory vesicles and gelatinase granules (23). Hence, exocytosis of specific and azurophil granules upon *P. stomatis* challenge was measured by the increase of plasma membrane expression of CD66b and CD63, respectively. A significant increase of CD66b expression was triggered by *P. stomatis* challenge compared to fMLF (Fig. 7A). The two oral pathogens *P. stomatis* and *P. gingivalis* triggered a similar increase of CD66b plasma membrane expression, which was significantly higher than basal levels (Fig. 7B). Figure 7C shows that *P. stomatis* challenge also resulted in a significant increase of CD63 plasma membrane expression, which was dependent on bacterial dose. Thus far, our data

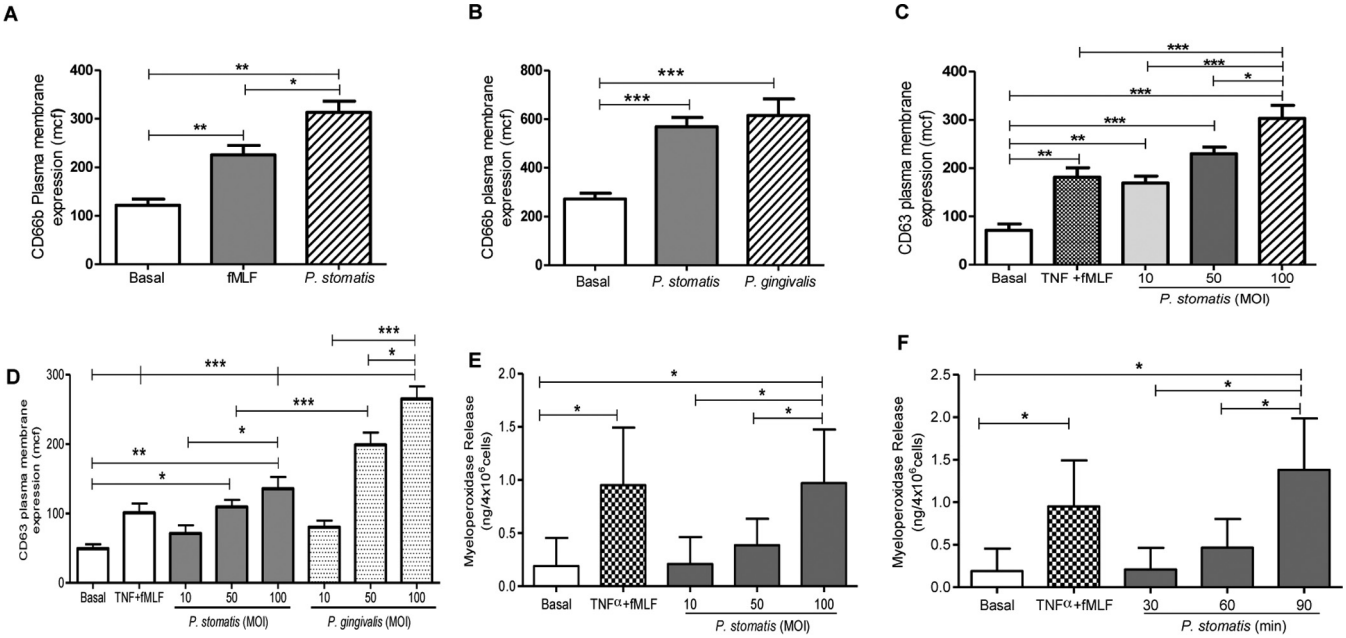

FIG 7 *P. stomatis* challenge induced specific granule exocytosis and a time- and bacterial-concentration-dependent azurophil granule release. Neutrophils were unchallenged (basal) or challenged with fMLF (5 min), with *P. stomatis* for 30, 60, or 90 min (MOI, 10), or with different *P. stomatis* or *P. gingivalis* MOIs (10, 50, or 100) for 30 min, or pretreated with TNF-α (10 min) followed by fMLF (TNF-α + fMLF). (A to D) Specific and azurophil granule exocytosis activities were quantified by the increase in plasma membrane expression of CD66b or CD63, respectively, by flow cytometry. Data are expressed as the means ± SEM of the mean channel of fluorescence (mcf) from 6 independent experiments (A), 5 independent experiments (B and D), or 10 independent experiments (C). (E and F) Supernatants from all the different experimental conditions were collected, and the release of myeloperoxidase to determine azurophil granule exocytosis was measured by ELISA. Data are expressed as means ± SEM of MPO release in nanograms per 4×10^6 cells from 5 independent experiments. *, $P < 0.05$; **, $P < 0.001$; ***, $P < 0.0001$.

showed that *P. stomatis* and *P. gingivalis* demonstrate similar ability to induce secretory vesicles and specific granule exocytosis, but *P. stomatis* was able to induce the release of higher levels of active gelatinase/MMP-9 than *P. gingivalis*. However, *P. gingivalis* induced a significantly higher increase of CD63 plasma membrane expression than *P. stomatis* at MOIs of 50 and 100 (Fig. 7D). To further confirm the exocytic ability of *P. stomatis* toward azurophil granule mobilization, the levels of myeloperoxidase (MPO), a major enzyme present in the matrix of azurophil granules, were determined. Similar to the flow-cytometric results, levels of MPO increased in a bacterial-dose-dependent manner (Fig. 7E). In addition, longer exposure between neutrophils and *P. stomatis*, at an MOI of 10, triggered a time-dependent increase of MPO levels (Fig. 7F). Collectively, these results demonstrate that *P. stomatis* interaction with human neutrophils triggered a robust exocytosis of the four different neutrophil granule subtypes.

DISCUSSION

High-throughput sequencing analyses have revealed that the composition of the oral microbiome from healthy and diseased periodontal sites is very diverse and that shifts from a symbiotic to a dysbiotic community occur as the disease progresses (7–10). Species such as *P. stomatis* that are detected with higher frequency in periodontal disease sites than in healthy sites are emerging as periodontal pathogens (10, 12, 14).

Neutrophils are the main innate immune cell present in the oral cavity, and interactions with the oral microbial community are critical in both oral health and disease (16, 32). Periodontal pathogens have the capacity to evade or manipulate neutrophil functional responses to promote inflammation (36). The goal of the present study was to begin to characterize the potential pathogenic profile of *P. stomatis* in the context of interactions with human neutrophils. We found that *P. stomatis* is resistant to neutrophil phagocytosis both when unopsonized and when opsonized with human serum. Oxygen-independent mechanisms were primarily responsible for killing engulfed as well as extracellular bacteria, and *P. stomatis* induced robust degranulation of

the four neutrophil granule subtypes. The significant decrease in extracellular bacterial survival after 120 min of challenge most likely could be attributed to the stimulated exocytosis of antimicrobial components found in neutrophil granules. Our results strongly indicate that proteins and/or peptides present inside neutrophil granules have antimicrobial properties toward *P. stomatis*, and studies to examine this are under current investigation in our laboratory.

In periodontal disease, activated neutrophils traffic from the blood into the gingival tissue to control microbial challenge, and during that journey oxygen radicals as well as antimicrobial peptides that can contribute to tissue damage are released (2, 16, 37). Periodontal pathogens have been shown to enhance the release of oxygen radicals. For example, dentilisin, a protease released from *T. denticola*, is involved in generation of ROS by human neutrophils through activation of complement (38). Neutrophil interaction with another oral pathogen, *Fusobacterium nucleatum*, results in high intracellular as well as extracellular ROS production (39). Both *T. denticola* and *F. nucleatum*, in the absence of opsonization, are efficiently internalized by neutrophils (40). *P. stomatis*, in the absence of serum opsonization, induced a robust intracellular ROS production, similar to that reported for other oral bacteria, albeit *P. stomatis* exhibits a low phagocytic uptake. The fusion of azurophil granules to *P. stomatis*-containing phagosomes would contribute to the high intracellular ROS detected by flow cytometry. Additionally, in another Gram-positive pathogen, *Listeria monocytogenes*, peptidoglycan induces high ROS production in neutrophils through activation of TLR2 (41). Therefore, it is possible that bacterial components, such as peptidoglycan and/or the peritrichous flagella, through activation of TLR2 and/or TLR5, could be responsible for the robust intracellular ROS generation. Studies to determine which neutrophil receptor(s) is involved in *P. stomatis*-induced neutrophil activation are under way in our laboratory.

Activation of the NADPH oxidase is initiated upon phagocytosis of microbial pathogens with the generation of superoxide radicals, which are quickly converted to hydrogen peroxide. In addition, the phagocytic vacuole is enriched by microbicidal peptides derived from the matrix of the different neutrophil granules upon fusion with the phagosome (18, 19). Hence, both oxygen-dependent and -independent mechanisms combine to ensure an efficient microbicidal environment inside the neutrophil phagosome (18). Several oral pathogens are protected against neutrophils' oxidative antimicrobial killing by the presence of enzymes such as superoxide dismutase, catalase, and rubrerythrin (42, 43). In the current study, neutrophils mounted a robust intracellular respiratory burst upon phagocytosis of *P. stomatis*; however, this antimicrobial response was not the main contributor to bacterial killing, since blocking the NADPH oxidase did not enhance *P. stomatis* survival. Moreover, the antimicrobial capacity toward *P. stomatis* from CGD neutrophils, which have impaired ability to generate ROS, was similar to the response observed by neutrophils with a functional NADPH oxidase. Phagosome maturation is accomplished in neutrophils by recruitment and fusion of specific and azurophil granules. Fusion of specific granules to bacterium-containing phagosomes results in the delivery of antimicrobial components, such as lactoferrin, to the phagosome. In our study, more than 50% of *P. stomatis* phagosomes recruited specific granules, as visualized by the granule marker lactoferrin. The lactoferrin-positive integrative pattern observed on *P. stomatis* phagosomes is an indication of granule fusion (31). Host proteins like lactoferrin can sequester iron, an important bacterial nutritional metal, and prevent microbial growth. It is possible that lactoferrin contributes to *P. stomatis* killing by inhibiting bacterial growth. Myeloperoxidase, present in the matrix of azurophil granules, is a key enzyme that uses hydrogen peroxide as a substrate to generate the toxic antimicrobial component hypochlorous acid (HOCl) (44). Our data showed that both specific and azurophil granules were efficiently recruited to *P. stomatis* phagosomes. Most likely, the fusion with and release of antimicrobial components, found in neutrophil granules, into the bacterial phagosome are the main contributors to *P. stomatis* decreased survival.

Chronic inflammation, as observed in periodontitis, is associated with increased

levels of reactive oxygen radicals produced mainly by the high number of neutrophils in their attempt to control the dysbiotic bacterial challenge (2). The generation of ROS contributes to periodontal tissue damage and also to osteoclast activation (42). Circulating neutrophils from periodontitis patients display higher basal ROS production than those from healthy matched controls (32). Moreover, patient neutrophils challenged *ex vivo* with *F. nucleatum* or *P. gingivalis* display an enhanced extracellular ROS release, which indicates that those cells have a primed neutrophil phenotype (45). Cytokines and bacterial products can prime neutrophils for an enhanced respiratory burst response, which can augment the cell antimicrobial efficiency but can also contribute to tissue damage. Our study shows that *P. stomatis* challenge of human neutrophils did not result in the direct generation of superoxide release; however, the bacterium was able to prime the fMLF-stimulated respiratory burst. These observations indicate that *P. stomatis* has the ability to prime human neutrophils. Studies in the gut show that the production of ROS generated during inflammation, mainly by infiltrated neutrophils, provides a source of exogenous electron acceptors, which benefits the growth of some pathogenic microbial species (46). It is interesting to speculate that in the gingival pocket *P. stomatis* could contribute to maintaining high levels of ROS by priming neutrophils and help sustain a source of electron acceptors, which might benefit its growth and/or facilitate the growth of other members of the oral dysbiotic microbial community.

Neutrophils have four different types of granules, and their release is hierarchical and tightly regulated, with secretory vesicles being the most easily mobilizable and azurophil granules the last to be released. The actin cytoskeleton, microtubules, and the small GTPases are involved in different steps of granule trafficking, with different SNARE proteins involved in final membrane fusion events (28, 47). Degranulation of neutrophils with release of toxic antimicrobial cargo into the extracellular space contributes to the tissue damage observed during the course of periodontal disease. High levels of matrix metalloproteinases, such as MMP8 and MMP9, mainly derived from the neutrophil granule pool, are found in the crevicular fluid of periodontitis patients (48). Oral pathogens such as *F. nucleatum*, *P. gingivalis*, and *T. denticola* trigger the release of MMP9 from stimulated neutrophils, with *P. gingivalis* showing minimal levels of the 92-kDa band, due to its high proteolytic activity, compared to the other two oral pathogens (40). In our study, *P. stomatis* induced a time-dependent release of MMP9 from human neutrophils that was significantly higher than the response induced by fMLF. In addition, the gelatin zymography gels showed higher levels of the 92-kDa band, corresponding to MMP9, in the supernatants collected from *P. stomatis*-challenged human neutrophils than in the supernatants collected from *P. gingivalis*-challenged neutrophils.

Recruitment and fusion of azurophil granules to bacterium-containing phagosomes are key events in neutrophil phagosome maturation due to the highly antimicrobial content present in this granule subtype. Myeloperoxidase, neutrophil elastase, proteinase 3, and other serine proteases are important components of azurophil granules, all of which have microbicidal properties (18, 19, 44). Azurophil granule exocytosis is tightly controlled, and only 20% of the granule pool is mobilized, since release of proteases from the cell will damage host tissues (24, 50). As with MMPs, elevated levels of MPO are present in the gingival crevicular fluid of periodontitis patients, indicating that oral pathogens can trigger azurophil granule exocytosis (51, 52). In this study, we found that *P. stomatis* challenge of human neutrophils triggered both a time-dependent and a concentration-dependent release of MPO. Similarly, *F. nucleatum*, *P. gingivalis*, and *T. denticola* can induce the release of elastase from neutrophils, and *Aggregatibacter actinomycetemcomitans* can induce MPO release (40, 51, 52). In contrast, we recently showed that the newly recognized periodontal pathogen *Filifactor alocis* did not induce azurophil granule release even at a high multiplicity of infection (53). Hence, various neutrophil responses may contribute to the pathogenic potential of different pathogenic bacteria.

A pool of azurophil granules, characterized by the presence of the small GTPase

Rab27a, localize close to the cell plasma membrane and undergo exocytosis instead of trafficking to the phagosome (54, 55). In our study, we observed by confocal staining of neutrophil elastase that azurophil granules were recruited to *P. stomatis* phagosomes and that the organism also induced exocytosis of this granule subtype. It is possible, therefore, that *P. stomatis* association with neutrophils triggers the mobilization of the Rab27a-positive subpopulation of azurophil granule.

In summary, we showed that *P. stomatis* is poorly phagocytosed by human neutrophils and that the internal bacteria are killed through oxygen-independent mechanisms, likely by recruitment of azurophil granules to the bacterium-containing phagosome. *P. stomatis* can prime neutrophils for an enhanced extracellular superoxide release upon subsequent stimulation. In addition, *P. stomatis* can induce robust mobilization of all four neutrophil granules with significant release of both MMP9 and MPO. The release of neutrophil granule content likely contributes to the significant extracellular killing of *P. stomatis* by neutrophils observed after 120 min. Overall, our data reveal that the emerging oral pathogen *P. stomatis* may limit its uptake by human neutrophils while promoting cell activation, which could contribute to damaging the host tissue.

MATERIALS AND METHODS

Human neutrophil isolation. Neutrophils were isolated from healthy human donors and one individual with autosomal chronic granulomatous disease (CGD) using plasma-Percoll gradients (28) and in accordance with the guidelines approved by the Institutional Review Board of the University of Louisville. Microscopic evaluations of the isolated cells, using Wright staining (ENG Scientific, Inc.), showed that >90 to 95% of the cells were neutrophils. Trypan blue exclusion indicated that >97% of cells were viable.

Bacterial strains and growth conditions. *P. stomatis* strain CM2 was cultured anaerobically at 37°C in tryptic soy broth supplemented with 20 g/liter yeast extract, 1% hemin, and 1% reducing agent (37.5 g/liter NH_4Cl, 25 g/liter $MgCl_2{\cdot}6H_2O$, 5 g/liter $CaCl_2{\cdot}2H_2O$, 50 g/liter L-cysteine HCl, 5 g/liter $FeCl_2{\cdot}4H_2O$). Nonviable bacteria were prepared by 90% isopropanol treatment under aerobic conditions for 10 min at room temperature. In order to remove residual isopropanol, the bacteria were washed twice in phosphate-buffered saline (PBS) buffer. Nonviability was confirmed by incubation in broth at 37°C for 24 h. For fluorescence assays, *P. stomatis* was labeled either with DAPI (10 μg/ml) or with CFSE (0.25 mg/ml) for 30 min at room temperature in the dark, and the cultures were washed 3 times with PBS prior to use. *Porphyromonas gingivalis* ATCC 33277 was cultured anaerobically at 37°C in Trypticase soy broth supplemented with yeast extract (1 mg/ml), hemin (5 μg/ml), and menadione (1 μg/ml).

Phagocytosis of *P. stomatis* by human neutrophils. (i) Imaging flow cytometry. Isolated human neutrophils (4×10^6 cells/ml) were unstimulated or challenged either with human serum-opsonized or with nonopsonized CFSE-labeled *P. stomatis* at a multiplicity of infection (MOI) of 10 (unless otherwise noted). As a control, neutrophils were challenged with either human serum-opsonized or nonopsonized Alexa Fluor 488 heat-killed *Staphylococcus aureus* (Invitrogen) (MOI, 10). Cells were incubated in a shaking water bath at 37°C for 30 min or 120 min and then rinsed with 0.05% sodium azide and fixed with 1% paraformaldehyde. Images were obtained, quantified, and visualized using an Amnis ImageStream^X (Millipore). Labeled bacterial internalization was detected using excitation with a 488-nm solid-state laser (channel 2), and the bright-field microscopy images were detected in channel 1. A total of 1,000 neutrophil events were collected per condition and sorted into bacterium-positive or -negative bins based on CFSE/Alexa Fluor 488 intensity. The data were analyzed using the IDEAS Application v6.0 software (Amnis-Millipore). For each experiment, the internalization wizard was used to design a mask to count the CFSE- or Alexa Fluor 488-positive cells and to ignore positive signals from membrane-associated or extracellular bacteria.

(ii) Confocal microscopy. Isolated human neutrophils (2×10^6 cells/ml) were stimulated with CFSE-labeled *P. stomatis* at an MOI of 10 and incubated in a shaking water bath at 37°C for 30 min. After incubation, the samples were rinsed once with RPMI medium, transferred to plates containing plasma-coated coverslips, and centrifuged at 600 $\times$ *g* for 8 min at 4°C. Cells were fixed with 10% formalin, and wheat germ agglutinin (WGA; Invitrogen) was used as a plasma membrane marker. Images were acquired by a Fluoview FV1000 confocal microscope and analyzed by FV-10ASW software (Olympus). To quantify the percentage of infection, 100 neutrophils were examined per condition, and the percentages of cells with bacteria internalized, attached to the plasma membrane, or both were calculated.

BacLight assay. The combination of two DNA dyes, Sytox Green and DAPI, was used to determine bacteria viability associated with human neutrophils as previously described (21). Human neutrophils (2×10^6 cells/ml) were challenged with DAPI-labeled nonviable *P. stomatis* (as a control) or with DAPI-labeled viable *P. stomatis* or with both DPI (10 μM; Sigma)- and DAPI-labeled *P. stomatis* in a shaking water bath at 37°C for 30 min or 120 min. At each time point, the samples were transferred to plates containing plasma-coated coverslips and centrifuged at 600 $\times$ *g* for 8 min at 4°C. The membrane-impermeable dye Sytox Green (0.4 μM) in 0.1 MOPS (morpholinepropanesulfonic acid) (pH 7.2)–1 mM $MgCl_2$ was added to detect bacterial cells with a compromised cell membrane. Confocal images were acquired within 30 min using a Fluoview FV1000 confocal microscope and analyzed by FV-10ASW

software. Quantification was performed by counting the total viable and nonviable bacteria both intracellularly and extracellularly from 200 neutrophils in 3 independent experiments.

Intracellular respiratory burst response. Isolated human neutrophils (4×10^6 cells/ml) were challenged with *P. stomatis* or with *S. aureus* at an MOI of 10 for 15 min or 30 min. The phagocytosis-stimulated respiratory burst response was measured by 2′, 7′-dichlorofluorescein (DCF; 5 μM) and analyzed by flow cytometry using a BD FACSCalibur as previously described (28). The nitroblue tetrazolium (NBT) assay was also used to visualize intracellular superoxide radical production induced by *P. stomatis*. Neutrophils (1×10^6 cells/ml) attached to plasma-coated glass coverslips were unstimulated or stimulated with *S. aureus* or with *P. stomatis*. Phagocytosis was synchronized at $600 \times g$ and 14°C for 4 min, and cells were incubated at 37°C in 5% CO_2 for 60 min in RPMI containing NBT. After incubation, cells were fixed with methanol and analyzed by light microscopy. Reduced NBT precipitates were visualized as blue formazan deposits.

Extracellular respiratory burst response. Human neutrophils (4×10^6 cells/ml) were left unstimulated or were challenged with fMLF (300 nM; Sigma) for 5 min or with *P. stomatis* for 5, 15, or 30 min at 37°C. For neutrophil priming assays, neutrophils were pretreated with TNF-α (2 ng/ml) for 10 min or with *P. stomatis* for 10 min, followed by stimulation with fMLF (300 nM) for 5 min. After stimulation, the samples were centrifuged for 10 min at $600 \times g$ and 4°C, and supernatants were collected. Superoxide anion release was measured spectrophotometrically at 550 nm as the superoxide dismutase-inhibitable reduction of ferricytochrome *c* as previously described (28).

Immunostaining of specific and azurophil granule recruitment. The fusion of specific and azurophil granules with bacterium-containing phagosomes was tested by immunostaining using confocal microscopy as previously described (21, 31). Human neutrophils (2×10^6 cells/ml) were settled on human serum-coated coverslips, incubated in RPMI 1640 with 10% fetal bovine serum, and unstimulated or challenged with CFSE-labeled *P. stomatis* or *S. aureus* for 30 min. Following treatment, samples were fixed in 10% formalin, permeabilized in acetone-methanol at −20°C, and blocked in PBS containing 5% bovine serum albumin for 1 h at room temperature. Recruitment of specific granules to bacterium-containing phagosomes was determined with anti-human lactoferrin primary antibody (MP Biomedicals). Azurophil granule recruitment was determined with anti-neutrophil elastase antibody (AHN-10; Millipore). The secondary antibody utilized was Alexa Fluor 555 (Life Technologies), and DAPI was used as a nuclear stain. Confocal images and z-stacks (1-μm thickness for each slice) were obtained using a Fluoview FV1000 confocal microscope with a 63× oil objective to determine specific and azurophil granule recruitment to bacterium-containing phagosomes. To quantify the enrichment of the bacterium-containing phagosomes for a granule subtype, 100 neutrophils were counted per condition, and if ≥50% of the phagosome was surrounded by lactoferrin or elastase, it was considered positive granule marker recruitment, as previously described (21).

Neutrophil granule exocytosis. Isolated human neutrophils (4×10^6 cells/ml) were suspended in buffer (basal) or stimulated with fMLF (300 nM) for 5 min or challenged with *P. stomatis* or *P. gingivalis* at an MOI of 10, 50, or 100 for 30 min; or they were pretreated with TNF-α (2 ng/ml; R&D Systems) for 10 min, followed by fMLF (300 nM) for 5 min. Exocytosis of azurophil granules, specific granules, and secretory vesicles was determined by measuring the increase in plasma membrane expression of membrane-associated receptors using antibodies: fluorescein isothiocyanate (FITC)-conjugated CD63 (clone AHN16.1/46-4-5; Ancell Corporation), FITC-conjugated anti human CD66b (clone G10F5; Biolegend), and phycoerythrin (PE)-conjugated anti-human CD35 (clone E11; Biolegend), respectively. After appropriate treatment, the samples were washed with 0.5% sodium azide, fixed with 1% paraformaldehyde, and analyzed by flow cytometry using a BD FACSCalibur instrument as previously described (28). Extracellular releases of MMP-9 (a marker for gelatinase granule exocytosis) and myeloperoxidase (MPO; a marker for azurophil granule exocytosis) were measured in the neutrophil supernatants collected from the experimental conditions described above by MMP-9 (Boster) and MPO (Abcam) enzyme-linked immunosorbent assays (ELISAs) in accordance with the manufacturer's instructions. The activities of MMP-9 in the supernatants from the same experimental conditions were analyzed by gelatin zymogen assays. Briefly, gelatin zymography was performed by using a 9% SDS-PAGE gel saturated with 1 mg/ml gelatin (300 bloom; Sigma Chemical). Samples (10 μg) with equal protein concentration were loaded onto the gel and electrophoresed at a constant 100 V for 2.5 h. The gels were incubated for 1 h at room temperature in 2.5% Triton X-100, followed by an overnight incubation at 37°C in gelatinase substrate buffer (50 mM Tris, 10 mM $CaCl_2$, and 0.02% NaN_2 [pH 8.0]). The gels were stained with 0.5% Coomassie blue followed by subsequent destaining with 50% methanol. Densitometry of the 92-kDa band intensity was quantified using ImageJ software.

Statistical analysis. Statistical analysis was performed using Student's *t* test or one-way analysis of variance (ANOVA) with the posttest Tukey-Kramer multiple comparison using GraphPad Prism software. Differences were considered significant at *P* levels of <0.05.

ACKNOWLEDGMENTS

We thank Terri Manning for neutrophil isolation and Alison K. Criss for her advice and expertise with bacteria viability, BacLight, and neutrophil granule immunostaining assays.

We declare that no conflicting interests exist.

We thank the NIH/NIDCR for funding through DE017921 and DE011111 (R.J.L.) and Consejo Nacional de Ciencia y Tecnologia (CONACYT) (E.J.F).

REFERENCES

1. Eke PI, Dye BA, Wei L, Slade GD, Thornton-Evans GO, Borgnakke WS, Taylor GW, Page RC, Beck JD, Genco RJ. 2015. Update on prevalence of periodontitis in adults in the United States: NHANES 2009 to 2012. J Periodontol 86:611–622. https://doi.org/10.1902/jop.2015.140520.
2. Darveau RP. 2010. Periodontitis: a polymicrobial disruption of host homeostasis. Nat Rev Microbiol 8:481–490. https://doi.org/10.1038/nrmicro2337.
3. Sosroseno W, Herminajeng E. 1995. The immunopathology of chronic inflammatory periodontal disease. FEMS Immunol Med Microbiol 10:171–180. https://doi.org/10.1111/j.1574-695X.1995.tb00030.x.
4. Davé S, Van Dyke TE. 2008. The link between periodontal disease and cardiovascular disease is probably inflammation. Oral Dis 14:95–101. https://doi.org/10.1111/j.1601-0825.2007.01438.x.
5. Kaur S, White S, Bartold PM. 2013. Periodontal disease and rheumatoid arthritis: a systematic review. J Dent Res 92:399–408. https://doi.org/10.1177/0022034513483142.
6. Shub A, Swain JR, Newnham JP. 2006. Periodontal disease and adverse pregnancy outcomes. J Matern Fetal Neonatal Med 19:521–528. https://doi.org/10.1080/14767050600797749.
7. Hajishengallis G, Lamont RJ. 2012. Beyond the red complex and into more complexity: the polymicrobial synergy and dysbiosis (PSD) model of periodontal disease etiology. Mol Oral Microbiol 27:409–419. https://doi.org/10.1111/j.2041-1014.2012.00663.x.
8. Hajishengallis G, Lamont RJ. 2016. Dancing with the stars: how choreographed bacterial interactions dictate nososymbiocity and give rise to keystone pathogens, accessory pathogens, and pathobionts. Trends Microbiol 24:477–489. https://doi.org/10.1016/j.tim.2016.02.010.
9. Kistler JO, Pesaro M, Wade WG. 2015. Development and pyrosequencing analysis of an in-vitro oral biofilm model. BMC Microbiol 15:1–10. https://doi.org/10.1186/s12866-014-0320-5.
10. Kumar PS, Griffen AL, Moeschberger ML, Leys EJ. 2005. Identification of candidate periodontal pathogens and beneficial species by quantitative 16s clonal analysis. J Clin Microbiol 43:3944–3955. https://doi.org/10.1128/JCM.43.8.3944-3955.2005.
11. Murphy EC, Frick I-M. 2013. Gram-positive anaerobic cocci—commensals and opportunistic pathogens. FEMS Microbiol Rev 37:520–553. https://doi.org/10.1111/1574-6976.12005.
12. Sizova MV, Chilaka A, Earl AM, Doerfert SN, Muller PA, Torralba M, McCorrison JM, Durkin AS, Nelson KE, Epstein SS. 2015. High-quality draft genome sequences of five anaerobic oral bacteria and description of *Peptoanaerobacter stomatis* gen. nov., sp. nov., a new member of the family *Peptostreptococcaceae*. Stand Genomic Sci 10:37. https://doi.org/10.1186/s40793-015-0027-8.
13. Oren A, Garrity GM. 2016. List of new names and new combinations previously effectively, but not validly, published. Int J Syst Evol Microbiol 66:4299–4305. https://doi.org/10.1099/ijsem.0.001585.
14. Downes J, Wade WG. 2006. *Peptostreptococcus stomatis* sp. nov., isolated from the human oral cavity. Int J Syst Evol Microbiol 56:751–754. https://doi.org/10.1099/ijs.0.64041-0.
15. Ryder MI. 2010. Comparison of neutrophil functions in aggressive and chronic periodontitis. Periodontol 2000 53:124–137. https://doi.org/10.1111/j.1600-0757.2009.00327.x.
16. Scott DA, Krauss J. 2012. Neutrophils in periodontal inflammation. Front Oral Biol 15:56–83. https://doi.org/10.1159/000329672.
17. Kolaczkowska E, Kubes P. 2013. Neutrophil recruitment and function in health and inflammation. Nat Rev Immunol 13:159–175. https://doi.org/10.1038/nri3399.
18. Quinn MT, DeLeo FR, Bokoch GM. 2007. Neutrophil methods and protocols. Preface. Methods Mol Biol 412:vii–viii.
19. Nordenfelt P, Tapper H. 2011. Phagosome dynamics during phagocytosis by neutrophils. J Leukoc Biol 90:271–284. https://doi.org/10.1189/jlb.0810457.
20. Reference deleted.
21. Johnson MB, Criss AK. 2013. *Neisseria gonorrhoeae* phagosomes delay fusion with primary granules to enhance bacterial survival inside human neutrophils. Cell Microbiol 15:1323–1340. https://doi.org/10.1111/cmi.12117.
22. Herrero-Turrión MJ, Calafat J, Janssen H, Fukuda M, Mollinedo F. 2008. Rab27a regulates exocytosis of tertiary and specific granules in human neutrophils. J Immunol 181:3793–3803. https://doi.org/10.4049/jimmunol.181.6.3793.
23. Uriarte SM, Powell DW, Luerman GC, Merchant ML, Cummins TD, Jog NR, Ward RA, McLeish KR. 2008. Comparison of proteins expressed on secretory vesicle membranes and plasma membranes of human neutrophils. J Immunol 180:5575–5581. https://doi.org/10.4049/jimmunol.180.8.5575.
24. Borregaard N, Sørensen OE, Theilgaard-Mönch K. 2007. Neutrophil granules: a library of innate immunity proteins. Trends Immunol 28:340–345. https://doi.org/10.1016/j.it.2007.06.002.
25. Sengelov H, Kjeldsen L, Borregaard N. 1993. Control of exocytosis in early neutrophil activation. J Immunol 150:1535–1543.
26. Reference deleted.
27. Matthews JB, Wright HJ, Roberts A, Ling-Mountford N, Cooper PR, Chapple ILC. 2007. Neutrophil hyper-responsiveness in periodontitis. J Dent Res 86:718–722. https://doi.org/10.1177/154405910708600806.
28. Uriarte SM, Rane MJ, Luerman GC, Barati MT, Ward RA, Nauseef WM, McLeish KR. 2011. Granule exocytosis contributes to priming and activation of the human neutrophil respiratory burst. J Immunol 187:391–400. https://doi.org/10.4049/jimmunol.1003112.
29. Allen L-AH, Beecher BR, Lynch JT, Rohner OV, Wittine LM. 2005. *Helicobacter pylori* disrupts NADPH oxidase targeting in human neutrophils to induce extracellular superoxide release. J Immunol 174:3658–3667. https://doi.org/10.4049/jimmunol.174.6.3658.
30. Lee J-W, O'Brien CN, Guidry AJ, Paape MJ, Shafer-Weaver KA, Zhao X. 2005. Effect of a trivalent vaccine against *Staphylococcus aureus* mastitis lymphocyte subpopulations, antibody production, and neutrophil phagocytosis. Can J Vet Res 69:11–18.
31. Monfregola J, Johnson JL, Meijler MM, Napolitano G, Catz SD. 2012. Munc13-4 protein regulates the oxidative response and is essential for phagosomal maturation and bacterial killing in neutrophils. J Biol Chem 287:44603–44618. https://doi.org/10.1074/jbc.M112.414029.
32. Uriarte SM, Edmisson JS, Jimenez-Flores E. 2016. Human neutrophils and oral microbiota: a constant tug-of-war between a harmonious and a discordant coexistence. Immunol Rev 273:282–298. https://doi.org/10.1111/imr.12451.
33. Condliffe AM, Kitchen E, Chilvers ER. 1998. Neutrophil priming: pathophysiological consequences and underlying mechanisms. Clin Sci 94:461–471. https://doi.org/10.1042/cs0940461.
34. Hurtado-Nedelec M, Makni-Maalej K, Gougerot-Pocidalo MA, Dang PM, El-Benna J. 2014. Assessment of priming of the human neutrophil respiratory burst. Methods Mol Biol 1124:405–412. https://doi.org/10.1007/978-1-62703-845-4_23.
35. Mair YH, Jhamb T, Visser MB, Aguirre A, Kramer JM. 2016. Sera and salivary matrix metalloproteinases are elevated in patients with vesiculoerosive disease: a pilot study. Oral Surg Oral Med Oral Pathol Oral Radiol 121:520–529. https://doi.org/10.1016/j.oooo.2016.01.002.
36. Olsen I, Hajishengallis G. 2016. Major neutrophil functions subverted by *Porphyromonas gingivalis*. J Oral Microbiol 8:30936. https://doi.org/10.3402/jom.v8.30936.
37. Miyasaki KT. 1991. The neutrophil: mechanisms of controlling periodontal bacteria. J Periodontol 62:761–774. https://doi.org/10.1902/jop.1991.62.12.761.
38. Yamazaki T, Miyamoto M, Yamada S, Okuda K, Ishihara K. 2006. Surface protease of *Treponema denticola* hydrolyzes C3 and influences function of polymorphonuclear leukocytes. Microbes Infect 8:1758–1763. https://doi.org/10.1016/j.micinf.2006.02.013.
39. Katsuragi H, Ohtake M, Kurasawa I, Saito K. 2003. Intracellular production and extracellular release of oxygen radicals by PMNs and oxidative stress on PMNs during phagocytosis of periodontopathic bacteria. Odontology 91:13–18. https://doi.org/10.1007/s10266-003-0022-1.
40. Ding Y, Haapasalo M, Kerosuo E, Lounatmaa K, Kotiranta A, Sorsa T. 1997. Release and activation of human neutrophil matrix metallo and serine proteinases during phagocytosis of *Fusobacterium nucleatum*, *Porphyromonas gingivalis* and *Treponema denticola*. J Clin Periodontol 24:237–248. https://doi.org/10.1111/j.1600-051X.1997.tb01837.x.
41. Remer KA, Reimer T, Brcic M, Jungi TW. 2005. Evidence of involvement of peptidoglycan in the triggering of an oxidative burst by *Listeria monocytogenes* in phagocytes. Clin Exp Immunol 140:73–80. https://doi.org/10.1111/j.1365-2249.2005.02740.x.
42. Chapple ILC, Matthews JB. 2007. The role of reactive oxygen and antioxidant species in periodontal tissue destruction. Periodontol 2000 43:160–232. https://doi.org/10.1111/j.1600-0757.2006.00178.x.
43. Sztukowska M, Bugno M, Potempa J, Travis J, Kurtz DM, Jr. 2002. Role of

rubrerythrin in the oxidative stress response of *Porphyromonas gingivalis*. Mol Microbiol 44:479–488. https://doi.org/10.1046/j.1365-2958.2002.02892.x.
44. Nauseef WM. 2014. Myeloperoxidase in human neutrophil host defence. Cell Microbiol 16:1146–1155. https://doi.org/10.1111/cmi.12312.
45. Matthews JB, Wright HJ, Roberts A, Cooper PR, Chapple IL. 2007. Hyper-activity and reactivity of peripheral blood neutrophils in chronic periodontitis. Clin Exp Immunol 147:255–264. https://doi.org/10.1111/j.1365-2249.2006.03276.x.
46. Rivera-Chávez F, Bäumler AJ. 2015. The pyromaniac inside you: *Salmonella* metabolism in the host gut. Annu Rev Microbiol 69:31–48. https://doi.org/10.1146/annurev-micro-091014-104108.
47. Ramadass M, Catz SD. 2016. Molecular mechanisms regulating secretory organelles and endosomes in neutrophils and their implications for inflammation. Immunol Rev 273:249–265. https://doi.org/10.1111/imr.12452.
48. Seguier S, Gogly B, Bodineau A, Godeau G, Brousse N. 2001. Is collagen breakdown during periodontitis linked to inflammatory cells and expression of matrix metalloproteinases and tissue inhibitors of metalloproteinases in human gingival tissue? J Periodontol 72:1398–1406. https://doi.org/10.1902/jop.2001.72.10.1398.
49. Reference deleted.
50. Sengelov H, Follin P, Kjeldsen L, Lollike K, Dahlgren C, Borregaard N. 1995. Mobilization of granules and secretory vesicles during in vivo exudation of human neutrophils. J Immunol 154:4157–4165.
51. Sheikhi M, Gustafsson A, Jarstrand C. 2000. Cytokine, elastase and oxygen radical release by *Fusobacterium nucleatum*-activated leukocytes: a possible pathogenic factor in periodontitis. J Clin Periodontol 2000 27:758–762.
52. Miyasaki KT, Nemirovskiy E. 1997. Myeloperoxidase isoform activities released by human neutrophils in response to dental and periodontal bacteria. Oral Microbiol Immunol 12:27–32. https://doi.org/10.1111/j.1399-302X.1997.tb00363.x.
53. Armstrong CL, Miralda I, Neff AC, Tian S, Vashishta A, Perez L, Le J, Lamont RJ, Uriarte SM. 2016. *Filifactor alocis* promotes neutrophil degranulation and chemotactic activity. Infect Immun 84:3423–3433. https://doi.org/10.1128/IAI.00496-16.
54. Munafo DB, Johnson JL, Ellis BA, Rutschmann S, Beutler B, Catz SD. 2007. Rab27a is a key component of the secretory machinery of azurophilic granules in granulocytes. Biochem J 402:229–239. https://doi.org/10.1042/BJ20060950.
55. Johnson JL, Brzezinska AA, Tolmachova T, Munafo DB, Ellis BA, Seabra MC, Hong H, Catz SD. 2010. Rab27a and Rab27b regulate neutrophil azurophilic granule exocytosis and NADPH oxidase activity by independent mechanisms. Traffic 11:533–547. https://doi.org/10.1111/j.1600-0854.2009.01029.x.